Numerical Simulations of Wind Induced Particle Contamination in Gypsum Landfill Surroundings

Matjaž Hriberšek, Niko Samec, Jure Ravnik & Matej Zadravec

Environmental Modeling & Assessment

ISSN 1420-2026
Volume 16
Number 5

Environ Model Assess (2011)
16:479-489
DOI 10.1007/s10666-011-9255-5

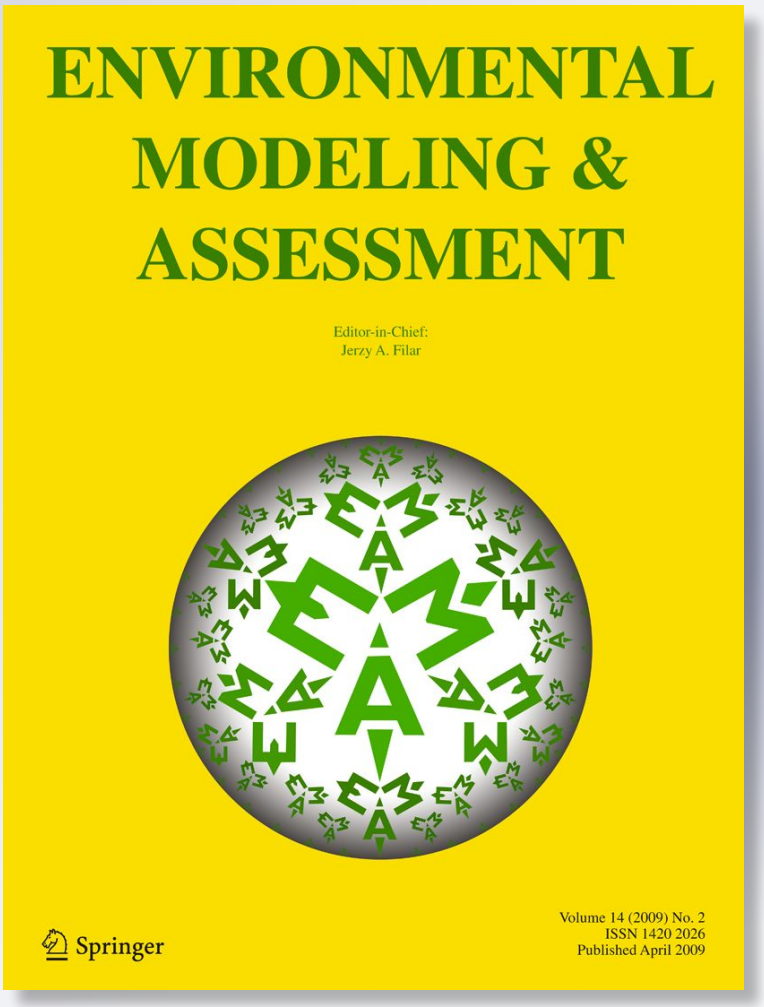

Springer

Environ Model Assess (2011) 16:479–489
DOI 10.1007/s10666-011-9255-5

Numerical Simulations of Wind Induced Particle Contamination in Gypsum Landfill Surroundings

Matjaž Hriberšek · Niko Samec · Jure Ravnik · Matej Zadravec

Received: 24 March 2010 / Accepted: 14 February 2011 / Published online: 11 March 2011

Abstract The contribution presents numerical simulation of gypsum particles, lifting from a gypsum landfill. First, particle characteristics are presented, resulting from different technologies of gypsum depositing. Next, a laboratory experiment parameter validation tests are described, which served as a means of determination of mass flow of particles from the landfill. The background of the numerical simulations, used in the assessment of landfill impact on the environment, is also described. Simulations consist of two parts: simulation of a long term impact of the particles on the surrounding area, performed by implementation of the Gaussian dispersion model based computer code ISC3, and second, a CFD based simulation for assessing the flow and mass concentration fields in the vicinity of the landfill for several pre-selected flow cases. The results of both computational approaches are presented and compared. In the conclusions, a relation of the simulation results with existing environmental pollution levels is made, and recommendations for landfill management are drawn.

Keywords Gypsum landfill · Gaussian dispersion model · Computational fluid dynamics · Wind induced particle transport · Atmospheric dispersion models

1 Introduction

Dust clouds are one of the important environmental risks, especially, when they originate from the artificially made landfills of hazardous material. Since particles, forming dust, are generally very small, they are easily lifted from the landfill and transported into the surroundings. The precondition for resuspension must be an adequate velocity field in the vicinity of the landfill surface. In the case of landfill material manipulations additional mechanical effects can significantly increase the amount of lifted particles. In the long term, the most important source of strong velocity field near the surface are winds, therefore the position of a landfill must be always determined by the wind rose, valid for the area under consideration.

In the case of the present study, the landfill under consideration was an existing wet landfill of gypsum, where gypsum sludge is deposited in a lagoon. Gypsum landfills are frequently presenting environmental risks, especially when gypsum is a product of gas cleaning technology [1]. A wet landfill does not present any important environmental risk in terms of dust clouds, however, it does present a technical problem due to a low landfill space efficiency. In order to increase the overall mass of deposited gypsum in the landfill, techniques of dry, dewatered, deposition have to be implemented. This leads to a situation, in which there will be numerous situations of strong winds and loose solid particles on the landfill surface, creating dust clouds.

Since the impact of the reconstruction on the environment can be experimentally verified only after the reconstruction is finished, modeling approach to prediction of environmental hazards has to be taken [2]. In order to minimize the impact of the dry gypsum landfill on its surroundings, an extensive experimental and numerical study was carried out. The experimental part was used for determination of mass flows from the model landfill surface, as predicted to occur in reality, and for characterization of particle properties, especially size distribution and shapes. A similar approach was presented [3], where gaseous tracer dispersion from a model of a landfill was studied, and in the case of dust loss from conveyors [4]. The experimental findings can be used

M. Hriberšek · N. Samec · J. Ravnik (✉) · M. Zadravec
Faculty of Mechanical Engineering, University of Maribor,
Smetanova ul.17,
SI-2000, Maribor, Slovenia
e-mail: jure.ravnik@uni-mb.si

in establishing boundary and initial conditions for numerical simulations of tracer propagation. On the other hand, direct computations of dust lifting by means of numerical methods have also been performed [5].

Today, numerical models form the core of modern engineering simulation tools. They range from complex models, incorporating governing physical phenomena of fluid flow and mass transfer on differential level, to simplified models, based on lumped parameter approach and with simplified solutions for fluid flow and mass transfer. In the case of modeling of dust clouds and the deposition of particles, complex models, based on Computational Fluid Dynamics (CFD), produce detailed spatial results, but they can become computationally too demanding for simulating large time spans. The latter is the domain of simplified models, which however lack spatial resolution. Several research works already implemented the CFD approach. A comparison of a CFD based model against experimental results from several field experiments was presented previously [6]. Comparison of results using Gaussian dispersion based and CFD based numerical models was also presented [7, 8]. In the field of Gaussian plume models, the ISCST3 model for dispersion of chromite ore from residue site was studied [9]. The application of GIS based urban topology construction for CFD analysis was described previously [10]. When dealing with particles, a review article [11] gives a good review of different modeling methodologies, including CFD, for near and far field dispersion cases.

The main goal of research, presented in the paper, was to set up numerical models, which would be able to predict the impact of the gypsum landfill on its environment in terms of solid particles dispersion into the atmosphere. The results of the present investigation will serve as a basis for final technological tuning of process of transformation of the wet landfill into the dry landfill. Additionally, during the process, several monitoring stations will be set up, what will later allow a comparison of computed results with results under realistic environmental conditions, and the position of the stations will be determined based on the results of numerical simulations.

2 Particle Characteristics

Data on structure and size distribution of the gypsum particles is one of the most important physical parameters, needed in setting up the correct physical model for numerical simulation. The data was determined for different compositions of the dewatered and built in gypsum. The main three cases were the summer composition, a mix consisting of 1 to 1 ratio of both, the winter composition, consisting of fresh gypsum only, and the built in gypsum only.

In all cases the test samples of gypsum were prepared by simulating the wringing out the gypsum, as will be performed on the landfill. The simulation was carried out on a laboratory vacuum filter device, able to produce samples with liquid content <30%. The samples were then analyzed using the Mastersizer 2000 (Malvern Instruments Ltd.) measuring device for the size distribution of particles, and additionally investigated under optical and electron microscope for the shape characterization of particles. For the latter purposes, the Nikon stereoscopic microscope was used, which allowed us to see the samples at 20–126× magnification. Pictures were taken with a high-resolution Sony CCD video camera, computer controlled using the Lucia M (Nikon, Japan) image analysis software package.

In the process of building-in the gypsum on the active area of the landfill the surface will be exposed to mechanical loads, resulting from loading, transportation by vehicles and hardening of the surface. In order to asses the influence of mechanical loading on the structure of the landfill surface and to simplify modeling of particles lift off, a laboratory simulation was carried out under simplified conditions. A flat surface of dry gypsum was prepared. A heavy roller drove over the surface a few times to crumble the gypsum. The samples were additionally dried up in order to obtain a possible unfavorable starting condition for a mechanical loading of the samples. The result of the loading was crushing of the specimen surface and appearance of small particles. The impact of the wind was simulated by the use of a fan, that induced near surface wind velocities in the magnitude of 1–1.2 m/s, that were responsible for the resuspension of the particles. The tests took 100 min to complete. The relative humidity of the air was 28%, the temperature was 23°C. The lifted particles were collected downstream and analyzed for their total mass and properties, including the density, the size and the shape. The results, later included in simulations, are time averaged values. The average density of particles, dried at 45°C and 0,9% wet, for three different samples, was 2.39 g/cm^3, which is close to the nominal density of gypsum, i.e. density of $CaSO_4 \times 2H_2O$= 2.317 g/cm^3. The shape of the dried particles is presented in Fig. 1, with a close-up of a typical sample. It can be concluded, that the general shape is rectangular and the ratio of the length to the diameter is approximately 10. This data was later used in selecting an adequate empirical correlation for drag coefficient for a particle.

The results of the conducted tests showed that the built in gypsum had the lowest emission index. The emission index of built in gypsum (0.0021 g/sm^2) is more than an order of magnitude smaller than one of the fresh gypsum (0.06 g/sm^2). Also, we noticed that the emission index rises substantially when gypsum is crumbled by heavy machinery. In order to capture the worst scenario, a short time 10 min tests were performed for the mix composition, the results was an increase in the emission index (0.049 g/sm^2),

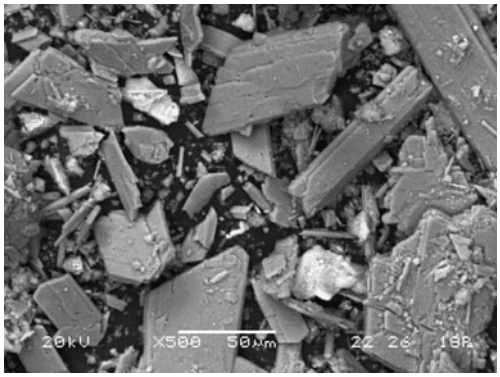

Fig. 1 Dry gypsum particles under the electron microscope

which was later used in numerical simulations. We anticipated, that in a long term view, which was the scope of our investigation, only conditions corresponding to mix and built-in compositions, would exist at the landfill, therefore the emission index of 0.049 g/sm^2 for the mix and 0.0021 g/sm^2 for the built-in compositions were used in numerical simulations.

In Table 1 the distribution of mass fractions for the typical size distribution classes of gypsum particles, after being exposed to mechanical loading, is presented. 24 samples were analyzed and the average size distribution is given in the second column of Table 1. We can see that the majority of particles fall in the category below 30 μm. In order to account for the effect of particles of different sizes, the size spectrum was divided into nine size classes, which were used in all numerical simulations. In order to test the sensitivity of numerical predictions on the increased values of the small particle fractions, one of the established size distributions of the samples with such a characteristic (third column in Table 1) was also included in the computations.

3 Numerical Models

We performed numerical simulations by using two types of numerical models, specifically:

1. Gaussian dispersion model, incorporated in the numerical code ISC- ISCST3 [12–14],
2. Computational Fluid Dynamics model (CFD), in our case in the form of the numerical code ANSYS-CFX [15].

There exist several other models, which were already successfully applied to environmental modeling [11, 16], especially Lagrangian models, incorporating lumped parameter approach with control volume movement according to predetermined flow field. Regardless of the numerical model used, the results of numerical simulations always depend strongly on input data, in our case:

1. Particle characteristics: size (equivalent diameter), size distribution, specific weight of wet and dry particles, characteristic shape and corresponding coefficient of dynamic drag.
2. Mass flow of particles, entering the flow domain as a consequence of wind interaction with landfill surface.
3. Direction and magnitude of winds in the surroundings of the landfill, mostly on several years average basis. In general, wind gusts should be considered, however, in this case, the numerical simulation would have to be time dependent, and more complex turbulence models (like LES) have to be applied in this case.

In the following, we will give a brief description of the numerical models used with special emphasis on selection of parameters and submodels.

3.1 Gaussian Dispersion Model

In Gaussian dispersion model the particle transport in the atmosphere is described by the steady state Gaussian plume model. In the case of ISC-AERMOD View software [14], which was used in the analysis, the Gaussian model is solved within the ISCST3 model. It uses the meteorological data for computing dispersion and deposition of particles in the general 3D domain, divided into computational cells.

Table 1 Size distribution of gypsum particles after the mechanical loading experiment

Particle equivalent diameter [μm]	Mass fraction (average) [%]	Mass fraction (severe case) [%]
5	38.7	52.9
15	16.5	25.2
25	7.5	7.9
35	6.6	3.9
45	3.8	3.1
60	6.0	1.7
85	5.8	1.6
150	9.6	2.3
320	5.5	1.4

The values were obtained by averaging the results of analysis of 24 samples

Inside each cell, the model calculates concentration and deposition flow for each hour as well as calculates average values for predefined time intervals. The model incorporates open pit source types, which corresponds to an open area of the gypsum landfill. It is also possible to simulate particle dispersion for several size classes simultaneously.

In order to qualitatively compare solutions of numerical modeling we take a look at the form of the steady state Gaussian plume model, describing concentration in the downwind (x) direction and cross flow (y) direction for each hour:

$$\chi = \frac{QVD}{2\pi u_s \sigma_y \sigma_z} \exp\left[-\frac{1}{2}\left(\frac{y}{\sigma_y}\right)^2\right], \tag{1}$$

with Q the mass flow rate (kg/s) of a certain size class, the $\sigma_y\sigma_z$ standard deviations of lateral and vertical concentration distribution, u_s the average wind velocity (constant within an hour), V the exponential decay term denoting vertical Gaussian concentration distribution and D exponential decay term describing chemical decomposition. The parameter σ_z is calculated as $\sigma_z=ax^b$, where parameters a and b are tabulated based on the Pasquill stability category [13]. Similarly, Briggs formulas are used to calculate σ_y, which is a function of downwind direction and stability category. Hourly values of atmospheric stability category are a part of the meteorological dataset needed to run the model. The vertical term V accounts for the vertical distribution of the Gaussian plume. It includes the effects of source elevation, receptor elevation, plume rise, limited mixing in the vertical, and the gravitational settling and dry deposition of particulates. In addition to the plume height, receptor height and mixing height, the computation of the vertical term requires the vertical dispersion parameter σ_z. The vertical term is calculated using a series of exponential terms depending of the receptor height and atmospheric mixing height. Detailed equations for the vertical term are given in [13]. The decay term was set to be equal 1, since no chemical decomposition of gypsum was considered in our work. During each hour, for which specific meteorological data is gathered, all parameters of Eq. (1) are assumed constant.

The particle concentration, which is of main interest in our study, is obtained by a double integration of Gaussian distribution function (1) in the downwind and crossflow direction:

$$\chi = \frac{Q_A}{2\pi u_s} \int_y \int_x \frac{VD}{\sigma_y \sigma_z} \exp\left[-\frac{1}{2}\left(\frac{y}{\sigma_y}\right)^2\right] dxdy, \tag{2}$$

with Q_A the area averaged mass flow. Lifting of particles for individual sizes Q_i is estimated using the equation:

$$Q_i = \varepsilon_i \phi_i Q, \tag{3}$$

where Q is the total flow and ϕ_i the mass fraction of each particle size category. The portion of the particles, which are lifted from the ground, is determined for each size category ε_i with the following equation:

$$\varepsilon_i = \frac{1}{1 + v_g/\alpha U_r}, \tag{4}$$

where ν_g is the gravitational settling velocity, U_r the wind velocity at 10 m height and α a constant that connects the flow from the open part of the landfill and a product of wind velocity and the concentration in the open part of the landfill. The value was determined by experiments α=0.029. The gravitational settling velocity is determined using the modified Stokes law:

$$v_g = \frac{(\rho - \rho_{air}) g d_p^2}{18\mu} S_{CF}, \quad S_{CF} = 1 + \frac{2x_2(a_1 + a_2 e^{-(a_3 d_p/x_2)})}{10^{-4} d_p} \tag{5}$$

where S_{CF} is the slip correction factor, ρ the particle density, ρ_{air} the air density, μ air viscosity, d_p the particle diameter, g the Earth's gravitational acceleration, while, x_2, a_1, a_2, a_3 are constants with values of 6.5×10^{-6}, 1.257, 0.4, and 0.55×10^{-4}, respectively. The model of particle settling on the surface determines the deposition F_d as the product of concentration χ_d and deposition velocity ν_d, calculated on the reference height z_d:

$$F_d = \chi_d v_d. \tag{6}$$

Concentration is calculated using Eq. (2). A resistance method is used to calculate the deposition velocity, v_d. The general approach used in the resistance methods for estimating v_d is to include explicit parameterizations of the effects of Brownian motion, inertial impaction, and gravitational settling. The deposition velocity is written as the inverse of a sum of resistances to pollutant transfer through various layers, plus gravitational settling terms [17, 18]:

$$v_d = v_g + \frac{1}{r_a + r_d + r_a r_d v_g}, \tag{7}$$

where r_a is the aerodynamical drag and r_d settling layer drag (s/m).

3.2 CFD Model

Dispersion of particles from the landfill can be also modeled by computing transport of particles in 3D turbulent flow of air in the vicinity of the landfill location. The CFD model enables modeling of transport of dangerous substances based on a given wind flow field and spatial geometry of the terrain. A digital GIS based model of heights was used to model the terrain surrounding the landfill.

A control volume based code Ansys-CFX 11.0 [15] was used. Reynolds averaged Navier–Stokes equations with two equation turbulence model were solved to predict turbulent flow around the landfill. This approach provides better accuracy than the Gaussian model, but it can be only employed for one instant of wind flow field and cannot provide long term averaged results. Several research works already implemented the CFD approach [6–8, 19].

The flow of air and the motion of particles were simulated by solving RANS equations. In order to include and compare the Euler-Euler (E-E) and Euler-Lagrangian (E-L) models, the two way coupling was considered in both cases. Therefore, the following equations were solved:

$$\frac{\partial \rho_f \phi_f}{\partial t} + \frac{\partial \rho_f \phi_f u_i}{\partial x_i} = 0, \tag{8}$$

$$\frac{\partial \rho_f \phi_f u_i}{\partial t} + \frac{\partial}{\partial x_j}\left(\rho_f \phi_f u_i u_j\right) = -\phi_f \frac{\partial p}{\partial x_i} + \phi_f \frac{\partial \tau_f}{\partial x_j} + f_{pi}, \tag{9}$$

$$m_p \frac{dv_i}{dt} = -F_{pi} = \frac{1}{8}\pi \rho_f d_p^2 C_D |w_i - v_i|(w_i - v_i) + \frac{1}{6}\pi d_p^3 \left(\rho_p - \rho_f\right) g_i + \frac{1}{4}\pi d_p^3 \nabla p, \tag{10}$$

where u_i is the air velocity component, p is the pressure, ρ_f is the air density, g_i the gravitational acceleration, ϕ is the volume fraction, t is time, d_p is the equivalent particle diameter, v_i is the particle velocity, ρ_p is the particle density and f_p is the interphase momentum exchange per unit volume. The velocity w_i is the air velocity, acting on a particle, obtained by additional implementation of turbulent particle dispersion model, see Eq. (13). Equations (8) and (9) are written for the continuous phase (air), in the same form equations for the dispersed phase were used in the case of the E-E model, with dynamic viscosity equal to viscosity of the continuous phase.

Comparing the forces acting on a particle, given in Eq. (10) and considered in both E-E and E-L simulations, the drag is the most important force. Aerodynamic lift and pressure gradient terms, included in Eq. (10), are in our case for gypsum particles with density much higher that the density of air negligible. Since the gypsum particles have a shape, that strongly differs from the sphere, for which the majority of standard correlations are valid, a physically more correct correlation for the drag coefficient had to be applied. Shape functions in the equation for the determination of the drag coefficient C_D were used [20] :

$$\frac{C_D}{K_2} = \frac{24}{\mathrm{Re}K_1K_2}\left[1 + 0.1118(\mathrm{Re}K_1K_2)^{0.6567}\right] + \frac{0.4305}{1 + \frac{3305}{\mathrm{Re}K_1K_2}} \tag{11}$$

Correlation is based on two shape function K_1 and K_2 and the particle Reynolds number *Re*. K_1 and K_2 are functions of sphericity ψ and are calculated based on the shape of the particles. Based on the experimental analysis of the shape of the particles, we determined that the particles are rectangular with length to diameter ratio of 10, leading to the value of sphericity ψ=0.6. The shape coefficients K_1 and K_2 were taken into account for each individual particle sizes. Based on the particle size distribution analysis, we focused our research on the nine size classes, presented in Table 1. The effect of turbulence on particles is accounted for by the Dispersed phase zero equation model for the E-E simulation, relating dispersed phase turbulent viscosity to continuous phase turbulent viscosity

$$\mu_{td} = \frac{\rho_p}{\rho_f}\frac{\mu_{tf}}{\sigma} \tag{12}$$

with σ the turbulent Prandtl number (set to 1). In case of the E-L simulation turbulent particle dispersion model [21] was used. It computes the fluctuating component of the air velocity

$$u_i' = \Gamma(2k/3)^{0.5} \tag{13}$$

with k local turbulent kinetic energy and Γ normally distributed random number. This velocity is added to the local mean air velocity u_i, determined from Eqs. (8) and (9), to obtain instantaneous air velocity w_i used in Eq. (10).

4 Computational Domain, Boundary and Initial Conditions

4.1 The Gaussian Plume Model

The modeling was done using the ISCST3 model, developed by the EPA [13, 14]. The model encompassed 100 km^2 around the gypsum landfill. The length of the model was 10,400 m and the width 10,400 m. Figure 2 shows terrain elevations, which were used in the model. A geodetic survey using a raster 25 m×25 m was preformed to obtain the elevations. The model requires data on the landfill as well. We chose the size of the open part of the landfill as 25×10 m, the landfill volume as 250 m^3 and its surface as 250 m^2. Particles are lifted from the bottom of the landfill, coefficients describing rinsing of gypsum in rain and snow were both set to 0.0001 (s mm/h)$^{-1}$.

The meteorological data was gathered from the two local stations for the period between 1.5.2003 and 19.11.2005. The first is located at the landfill measuring the temperature, precipitation and wind direction and velocity. The second is located in the nearby (6 km) town of Celje, where data on relative humidity, cloud cover, cloud height, sun

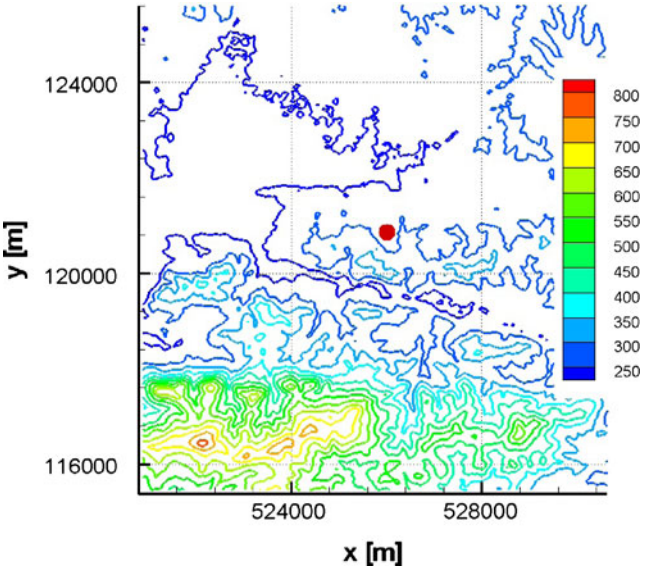

Fig. 2 Terrain height around the location of the landfill. Contours show height in meters above sea level. The landfill, shown with the dot, is located at 262.74 m

radiation and air pressure was gathered. The meteorological parameters were measured on an hourly basis and were recorded in a digital manner. The data was written in the SAMSON (Solar and Meteorological Surface Observational Network) format and a RAMMET [14] meteorological pre-processor was used to prepare data for our model. RAMMET requires also additional terrain data, in our case: anemometer height 2 m, minimum Monin-Obukhov length 2 m, surface roughness length (measurement site) 0.1 m, surface roughness length (application site) 0.1 m, noon-time Albedo 0.18, Bowen ratio 0.8, anthropogenic heat flux 43 W/m^2, fraction of net radiation absorbed at the ground 0.15. The AERMIX model [14] was used to estimate the mixing heights. Since the model has been run using actual measured meteorological data, atmospheric stability class was estimated using these data. The emission index values from experimental tests were used for computing the total mass flow from the landfill area and used as input to the Gaussian plume model (Eq. 5) together with size distribution, as presented in Table 1. The model was run on a grid of receptors. A combination of polar and equidistant distributions was used. It is shown in Fig. 3.

4.2 The CFD Model

The area under consideration encompassed 10.5 km times 10.5 km with the landfill located in the centre. This configuration was chosen in order to be able to select any wind direction without the necessity to construct a new mesh. The terrain elevations (Fig. 2) were used to set up the bottom surface of the computational domain. The upper boundary of the domain was flat, set 2,612 m above the lower point in the terrain, thus positioning the upper boundary at the elevation of the highest meteorological data point for wind profiles. The side walls of the domain were vertical. Based on the geometrical model two computational grids were set up having 434,000 elements and 2.1 million elements (Fig. 3). The grids were refined around the landfill, ensuring the landfill area was discretisized by elements with a typical size of 10 m. The boundary conditions were set as follows: Inflow of air was prescribed on two vertical walls in all computed cases and an outflow on the opposite two. On the top of the domain, the free slip condition was applied; on the bottom the no-slip condition was chosen. Based on the wind rose measurements three dominant wind directions were chosen to set up the CFD simulations. In Fig. 4, wind velocity profiles at the inlet for the preselected wind directions are given. Meteorological data was obtained from the Environmental Agency of Slovenia, originating from the meteorological station west of the landfill, which position corresponded with the inflow boundary of the domain. For the implementation as the inlet boundary conditions linear interpolation between the data points was used. The highest average monthly wind velocity was selected, in order to capture the worst case scenario in our model. At the outflow boundaries, fully developed flow conditions were assumed. Based on the

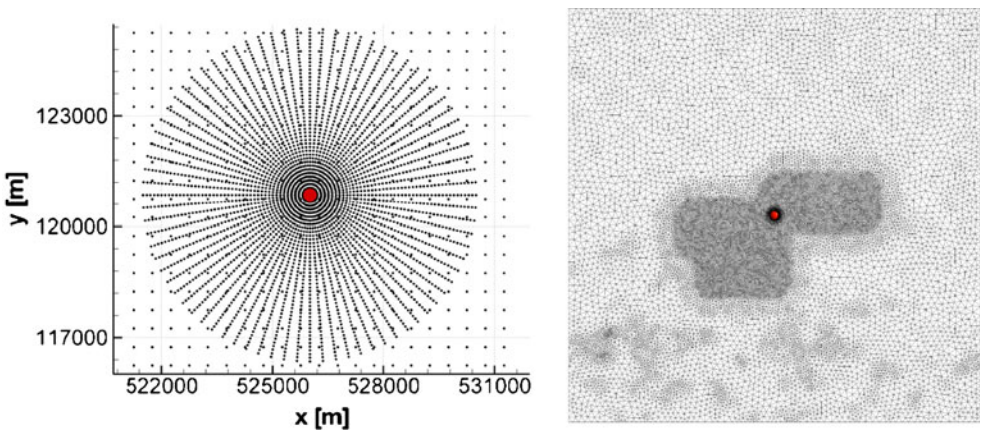

Fig. 3 Computational grids. Left receptor locations of the ISCST3 model, right dense mesh of the CFD model. Landfill location is shown with a dot

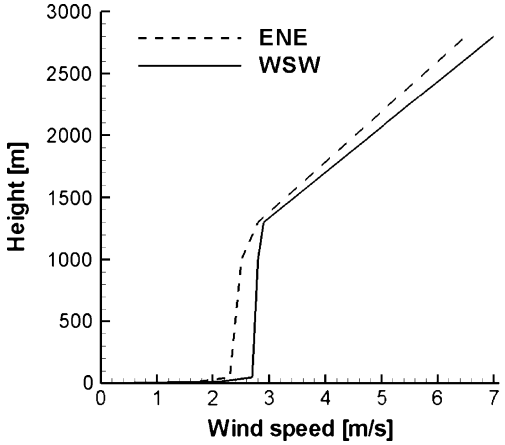

Fig. 4 Vertical wind profiles for the CFD model. In the ISCST3 model wind velocities at 10 m height were used, i.e. 1.7 m/s ENE and 2.1 WSW

measured emission index, within the elements at the landfill surface the gypsum mass sources were prescribed together with considering the size distribution of particles (Table 1). At the terrain surface, the particles, that hit the wall, were removed from computation, i.e. deposited on the ground.

Validation study was performed with respect to mesh density and choice of turbulence model. At the inlet, turbulence intensity level of 10% was set. The standard k-ε and the k-ω based SST [15] two-equation eddy viscosity models were tested. Both models are valid for fully developed steady state turbulent flow. The LES (Large Eddy Simulation) model would clearly be a better choice, since it would allow physically relevant computation of time-dependent flow (i.e. changing wind magnitude and direction), but at the expense of yet denser computational grids and small time steps, making LES currently out of reach considering computational demands for the presented case. Comparison of turbulent kinetic energy distribution showed that there are no major differences in the magnitude and spatial distribution, therefore the standard k-ε model was used in all particle dispersion computations.

When comparing results of flow field between both computational meshes in the direction of the main flow, Fig. 5, it is evident that the coarse mesh provides flow resolution very close to results of the dense mesh. Due to relatively short computational times the coarse mesh was therefore selected and used in all performed CFD simulations.

5 Results of Numerical Simulations

5.1 Gaussian Plume Model Used with a Meteorological Dataset

The Gaussian plume model ISCST3 was run with meteorological data between May 2003 and November 2005. Gypsum with density 2,210 kg/m^3 was chosen. Emission index of built in gypsum 0.0021 g/s/m^2 and mixed gypsum 0.049 g/s/m^2 was selected. The two gypsum diameter/mass fractions distributions (average case and severe case) used in the model are listed in Table 1.

Firstly, we ran simulations using average mass fraction distribution. The aim of this simulation was to predict worst case scenarios, corresponding to constant gypsum emissions from the landfill occurring during a long time period of meteorological conditions. Highest/worst concentrations throughout the period were chosen for analysis. Three hour averages are presented, which are representative of the problem, since averaging omits possible errors in the meteorological dataset, like short one-time events, that may have been recorded by the meteorological station. Figure 6 shows contours of constant gypsum concentration in the air, showing the worst 3 h averaged value in each individual node in the period May 2003–November 2005, for both values of emission index. We observe that the concentration decreases almost in concentric circles around the landfill. The predominant South-Western and North-Eastern wind direction is evident from the contours of low concentration, i.e. 100 μg/m^3. Figure 7 shows deposition of gypsum, also for worst 3 h averaged value in each individual node in the period May 2003–November

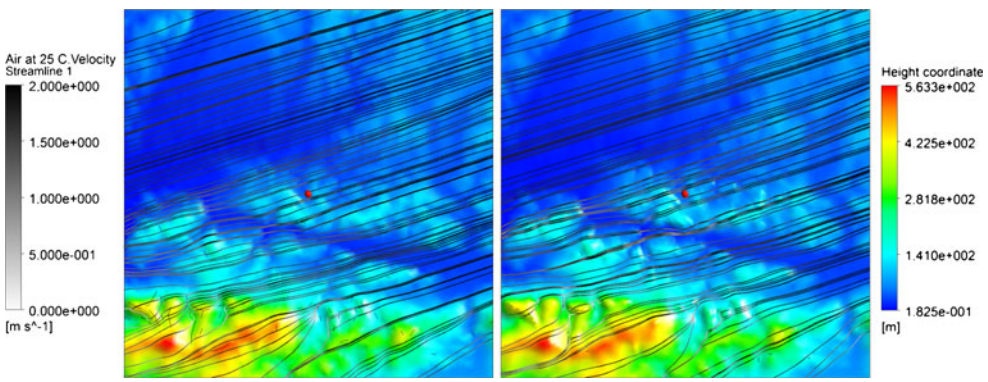

Fig. 5 Comparison of velocity streamlines: coarse mesh (left), dense mesh (right)

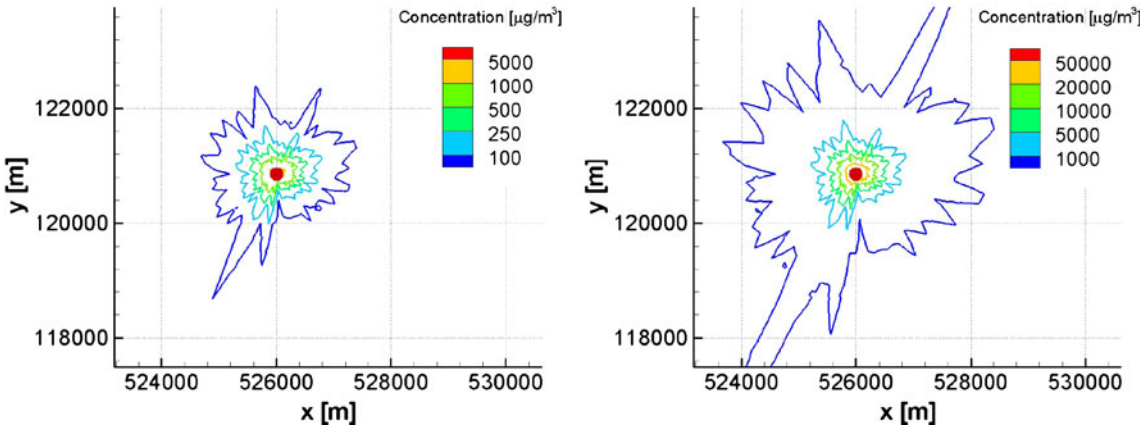

Fig. 6 Concentration contours from the real weather data simulation. Emission index 0.0021 g/s/m^2 (left) and 0.049 g/s/m^2 (right)

2005. In the case of emission index 0.049 g/s/m^2 the results show an increase in the concentration values but otherwise the same concentration pattern is recognizable.

We may conclude, that in the worst scenario case, we may expect one three hour period in two and a half years when 1 km away from the centre of the landfill the gypsum concentration in the air will reach about 250 μg/m^3 for the first case and about 5,000 μg/m^3 for the second emission case. When considering deposition of particles, at the same distance from the landfill about 0.1 g/m^2 of gypsum will be deposited on this day for the first case and 3 g/m^2 for the second emission case. The higher rates computed are attributed to extremely high particle emission rates (short time experiment), which are not likely to occur over a long time periods, therefore results for the lower emission index should be considered when estimating environmental impact on the surroundings.

5.2 Predominant Wind Directions

As stated earlier it is very difficult to directly compare the results between the ISCST3 model and CFD models, as the CFD models are limited to a fixed wind direction and magnitude. In order to be able to qualitatively and quantitatively compare both modeling approaches, we set a few test cases with fixed predominant wind direction. Vertical wind profiles, depicted in Fig. 4, were set as the inflow conditions for CFD (Euler-Euler and Euler-Lagrangian models), and in the Gaussian plume model the wind speed at 10 m height (1.7 m/s ENE and 2.1 m/s WSW) and its direction was imposed into the meteorological dataset.

Two wind directions and two emission indices were thus considered. In order to compare the 2D Gaussian plume results to 3D CFD simulation, we extracted the highest concentration values from vertical concentration profiles of the CFD simulation results. This enabled drawing of concentration contours on 2D field and a direct comparison to Gaussian plume results. Gypsum concentration contours for all three models are shown in Figs. 8 and 9 for emission index 0.049 g/s/m^2 and average particle size distribution. The concentration values presented are the cumulative values, i.e. include all nine size classes accounted for in the simulations.

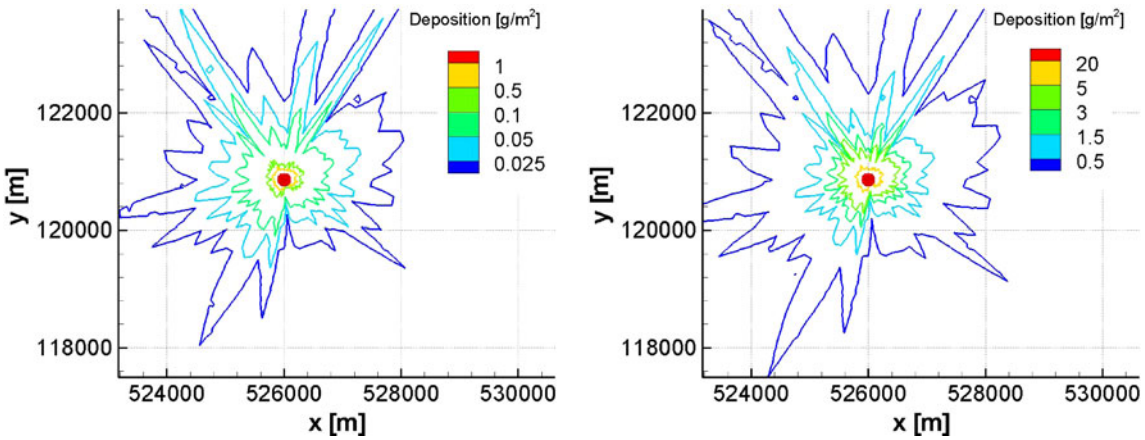

Fig. 7 Deposition contours from the real weather data simulation. Emission index 0.0021 g/s/m^2 (left) and 0.049 g/s/m^2 (right)

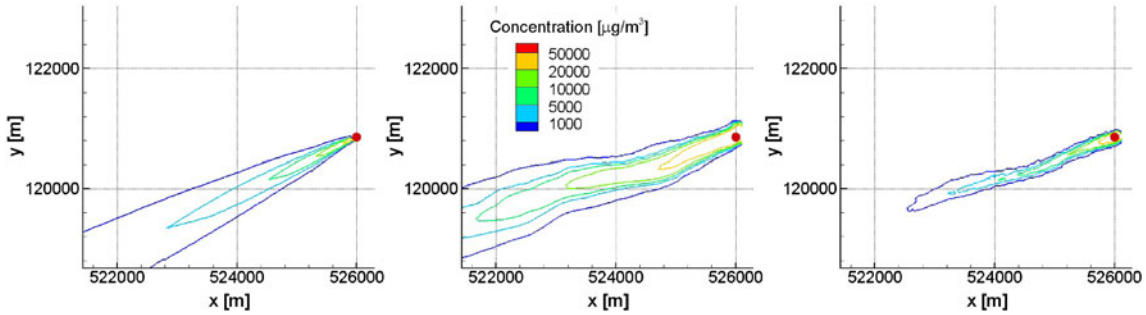

Fig. 8 Concentration contours for East-North-Eastern wind and emission index 0.049 g/s/m^2. Results of the ISCST3 model (left), CFD Euler-Euler model (middle) and CFD Euler-Lagrangian model (right) are shown. Landfill location is shown with a dot

Contours plots of selected emission index were generated using fixed contours values. We observed that in all cases the Euler-Lagrangian CFD model predicts a very narrow plume, in contrast to the Euler-Euler CFD model and Gaussian model, which predict a distinctly wider spread of gypsum. The difference in the width of the plume for the Euler-Euler CFD model is mainly attributed to the fact that the diffusion term in Eq. (9) of the Euler-Euler CFD model, includes molecular as well as turbulent dispersion. In the case of Euler-Lagrangian CFD model this is not the case, since turbulence dispersion model used depends only on characteristics of local turbulence field when computing fluctuating velocity, responsible for simulating dispersion in Lagrangian particle tracking algorithm. Therefore in all cases Euler-Lagrangian model under-predicted the plume width.

Looking at the contour shapes in the case of WSW wind (Fig. 9) we observe good agreement between Gaussian model and Euler-Euler model. The predicted concentration levels are very close as well as the dispersion of the pollutant in the direction perpendicular to the predominant wind. The distances from the landfill in the direction of the wind reached by each contour are also very close.

However, in the case of ENE wind we observe that CFD plume shifts away from the wind direction in the south-eastern part of the domain. This is caused by the hills that are located in that area (Fig. 2). Although the terrain elevations were present in the Gaussian plume model as well, the CFD model shows their influence better. In the north-east the terrain is flat thus the WSW wind drives the plume in the same direction for all three models, and the agreement between the results is significantly better.

The influence of the emission index and particle size distribution was studied using ISCST3 model. Concentration contours for average particle distribution and for severe case particle distribution for emission index 0.0021 g/s/m^2 and severe case for 0.049 g/s/m^2 are shown for WSW wind in Fig. 10.

Comparing the two emission indices, we observe that the influence of the increase in the number of particles on particle flow pattern was negligible. The shapes of concentration contours remain almost the same, only the levels change. This was expected for the Gaussian plume model, since the influence of particles on the flow is not modeled. In the CFD models the particles do exchange momentum with the flow; however the volume fraction occupied by the particles for both emission indices is still very small resulting in almost negligible momentum exchange with the air flow.

Comparing the average particle distribution and severe case particle distribution we can clearly observe that

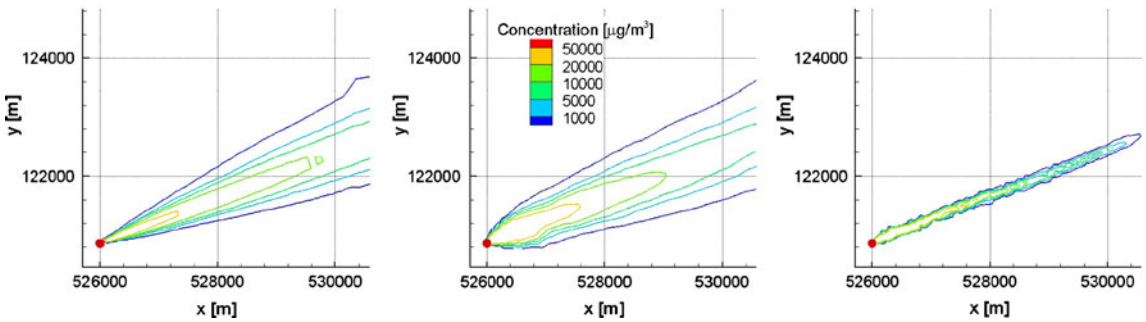

Fig. 9 Concentration contours for West-South-Western wind and emission index 0.049 g/s/m^2. Results of the ISCST3 model (left), CFD Euler-Euler model (middle) and CFD Euler-Lagrangian model (right) are shown. Landfill location is shown with a dot

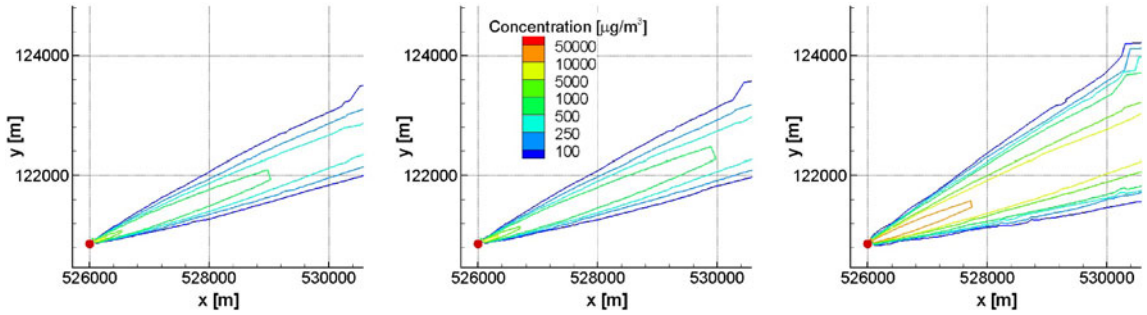

Fig. 10 Concentration contours simulated using ISCST3 model for West-South-Western wind. Emission index 0.0021 g/s/m^2. (left and middle), 0.049 g/s/m^2 (right). Average particle distribution (left), severe case (middle and right). Landfill location is shown with a dot

concentration levels are raised and the same contours encompass a larger area. This was expected, since the severe case particle distribution includes a larger mass fraction of the smallest particles, having the lowest settling velocity thus being able to travel the farthest. For example, in the case of WSW wind and emission index 0.0021 g/s/m^2, the 1,000 μg/m^3 contour reaches up to about 3.2 km from the landfill location in the average mass fraction case and up to about 4.2 km in the severe case.

Simulation of severe case of particle size distribution with real weather data is presented in Fig. 11 for emission index 0.049 g/s/m^2. In comparison with average particle size distribution (Figs. 6 and 7) we observe that the general contour pattern remains of the same shape. The highest concentration is still observed in the South-Western and North-Eastern wind directions. Comparing the concentration and deposition values, contours of the severe case reach larger distances from the landfill. This is due to the larger mass fraction of small particles, for which settling is the slowest. We may conclude that positioning of monitoring points could therefore be based on computational results for the average particle size distribution.

6 Conclusions

In the process of transformation of a wet gypsum landfill into a dry one environmental hazards of the process have to be evaluated in order to adapt the transformation procedures. As one of the hazards is dusting of dry particles due to strong winds, the goal of the presented research work was to find how dangerous this transformation process would be and how it will affect the surroundings of the landfill. As the meteorological influences are the most important in this case, computational study was performed.

Simulations confirmed our assumption that the wind direction and terrain characteristics are the main factors influencing the transport and distribution of gypsum particles. The highest concentration levels were found in the immediate surroundings of the landfill, but they diminished quickly as we move away from the landfill. Despite the lack of accuracy in flow resolution, the Gaussian model is able to produce reasonably accurate long term impact results with a moderate computational time. Results of the Euler-Euler CFD model and the Gaussian plume model were in good agreement when

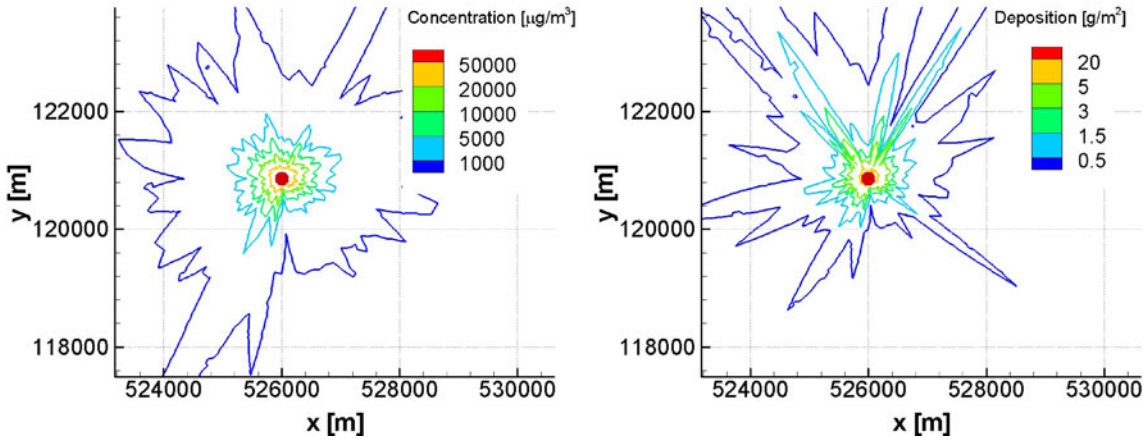

Fig. 11 Concentration (left) and deposition (right) contours simulated using ISCST3 model for real weather data and severe particle mass fraction distribution. Emission index 0.049 g/s/m^2. Landfill location is shown with a dot

plume was traveling over flat terrain. The influence of terrain elevations was captured better in the Euler-Euler CFD model, which is a result of a much better underlying theoretical basis of flow description. On the other hand, the long computational times of the Euler-Euler CFD model, when applied in the context of time dependent simulations with time span of several years, is currently still a clear drawback of the model. The Euler-Lagrangian simulation failed to capture realistic spreading of the particles, particularly in the cross-flow direction.

Since results of short time computations, presented in the paper, are comparable with CFD model results, this leads to the conclusion, that in the presented case the Gaussian model offers the best combination of short computational times with sufficient accuracy for evaluating the impact of the landfill on the surroundings. In order to test the sensitivity of the computational results to a change in volume fractions of the smallest particles a second particle size distribution with higher values of smallest particles fractions was tested in the Gaussian model. The results show almost the same concentration pattern with increased concentration values at larger distances from the landfill. The computational results can therefore serve as a basis for long term monitoring of spreading and deposition of particles in the surroundings of the gypsum landfill.

References

1. Plaza, C., Xu, Q., Townsend, T., Bitton, G., & Booth, M. (2007). Evaluation of alternative landfill cover soils for attenuating hydrogen sulfide from construction and demolition (C&D) debris landfills. *Journal of Environmental Management, 84*(3), 314–322.
2. Nazaroff, W. W., & Alvarez-Cohen, L. (2001). *Environmental engineering science*. John Wiley and Sons.
3. Carpentieri, M., Corti, A., & Zipoli, L. (2004). Wind tunnel experiments of tracer dispersion downwind from a small-scale physical model of a landfill. *Environmental Modelling and Software, 19*, 881–885.
4. Witt, P. J., Carey, K. G., & Nguyen, T. (2002). Prediction of dust loss from conveyors using computational fluid dynamics modelling. *Applied Mathematical Modelling, 26*, 297–309.
5. Klemens, R., Kosinski, P., Wolanski, P., Korobeinikov, V. P., Markov, V. V., Menshov, I. S., et al. (2001). Numerical study of dust lifting in a channel with vertical obstacles. *Journal of Loss Prevention in the Process Industries, 14*, 469–473.
6. Hanna, S. R., Hansen, O. R., & Dharmavaram, S. (2004). FLACS CFD air quality model performance evaluation with Kit Fox, MUST, Prairie Grass, and EMU observations. *Atmospheric Environment, 38*(28), 4675–4687.
7. Riddle, A., Carruthers, D., Sharpe, A., McHugh, C., & Stocker, J. (2004). Comparisons between FLUENT and ADMS for atmospheric dispersion modelling. *Atmospheric Environment, 38*(7), 1029–1038.
8. Mori, A. (2000). Integration of plume and puff diffusion models/ application of CFD. *Atmospheric Environment, 34*(1), 45–49.
9. Scott, P. K., & Proctor, D. (2003). Soil suspension/dispersion modeling methods for estimating health-based soil cleanup levels of hexavalent chromium at chromite ore processing residue sites. *Journal of Air and Waste Management*, *58*(3), March.
10. Chua, A. K. M., Kwokb, R. C. W., & Yua, K. N. (2005). Study of pollution dispersion in urban areas using Computational Fluid Dynamics (CFD) and Geographic Information System (GIS). *Environmental modelling & Software, 20*, 273–277.
11. Holmes, N. S., & Morawska, L. (2006). A review of dispersion modelling and its application to the dispersion of particles: an overview of different dispersion models available. *Atmospheric Environment, 40*(30), 5902–5928.
12. U. S. Environmental Protection Agency. (1995). *User's guide for the Industrial Source Complex (ISC3) dispersion models—volume 1 (Revised). EPA-454/B-95-003a*. Research Triangle Park: Office of Air Quality Planning and Standards.
13. U. S. Environmental Protection Agency. (1995). *User's guide for the Industrial Source Complex (ISC3) dispersion models—volume II—Description of model algorithms. EPA-454/B-95-003b*. Research Triangle Park: Office of Air Quality Planning and Standards.
14. ISC-AERMOD View. (2006). Interface for the U.S. EPA ISC and AERMOD Models, Lakes Environmental.
15. Ansys- 11.0. (2006). AEA Technology.
16. VDI 3783 Bl. 12 Entwurf. (1999). Umweltmeteorologie. Physikalische Modellierung von Stroemungs- uns Ausbreitungsvorgaengen in der atmosphaerischen Grenzschicht. Berlin: Beuth Verlag.
17. Slinn, S. A., & Slinn, W. G. N. (1980). Predictions for particle deposition and natural waters. *Atmospheric Environment, 14*, 1013–1016.
18. Pleim, J., Venkatram, A., & Yamartino, R. (1984). *ADOM/TADAP model development program. Volume 4. The dry deposition module*. Rexdale: Ontario Ministry of the Environment.
19. Gosman, A. D. (1999). Developments in CFD for industrial and environmental applications in wind engineering. *Journal of Wind Engineering and Industrial Aerodynamics, 81*(1–3), 21–39.
20. Ganser, G. H. (1993). A rational approach to drag prediction of spherical and nonspherical particles. *Powder Technology, 77*, 143–152.
21. Gosman, A. D., & Ioannides, E. (1981). Aspects of computer simulation of liquid fuelled combustors. *AIAA Paper*, No. 81–0323.